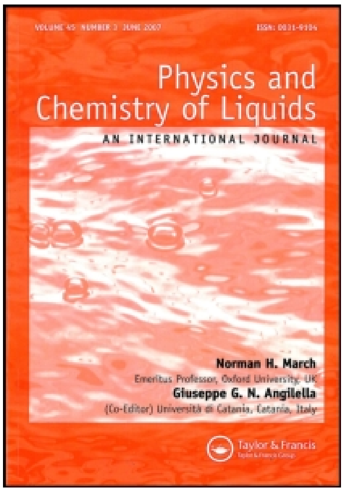

Physics and Chemistry of Liquids
Publication details, including instructions for authors and subscription information:
http://www.informaworld.com/smpp/title~content=t713646857

The structure of O/W microemulsions formulated with alkylglucosides

E. Acosta[a]; B. Ginzberg[a]; M. Bisceglia[a]; D. Kurlat[a]
[a] Departmento de Física, Facultad de Ingeniería, UBA, Paseo Colon 850, 1063-Buenos Aires, Argentina

To cite this Article Acosta, E. , Ginzberg, B. , Bisceglia, M. and Kurlat, D.(2005) 'The structure of O/W microemulsions formulated with alkylglucosides', Physics and Chemistry of Liquids, 43: 2, 115 — 122
To link to this Article: DOI: 10.1080/00319100420003035 45
URL: http://dx.doi.org/10.1080/00319100420003035 45

Physics and Chemistry of Liquids
Vol. 43, No. 2, April 2005, 115–122

The structure of O/W microemulsions formulated with alkylglucosides

E. ACOSTA, B. GINZBERG, M. BISCEGLIA and D. KURLAT*

Departmento de Física, Facultad de Ingeniería, UBA, Paseo Colon 850,
1063-Buenos Aires, Argentina

(*Received 5 July 2004*)

By following a method proposed by Kahlweit, an equilibrium diagram was determined in O/W quaternary microemulsions. These systems were formed by octanol (cosurfactant)/water/octane (oil)/alkylglucoside (surfactant). The experiment study was performed at two different temperatures (25°C and 50°C). The objective of this study work was to determine the structure of these lower microemulsions and to study the influence of the cosurfactant. Hence, different experimental techniques were employed: light scattering (static and dynamic), Kerr effect (static and dynamic), viscosity and refractometric measurements. It was concluded that the surfactant volume fraction in equilibrium with micelles is 0.044 and the micelle shapes are revolution ellipsoids.

Keywords: Microemulsions; Equilibrium diagrams; Alkyl polyglycosides

1. Introduction

As remarked earlier, microemulsion phase behaviours present several similarities irrespective of the differences in composition which these systems can present. These common characteristics have been systematized by means of the so-called Winsor diagrams (W). In this characterization they are presented under the sequence lower-phase microemulsion ($\underline{2}$ or WI) → middle-phase microemulsion (3 or WIII) → upper-phase microemulsion ($\overline{2}$ or WII). As it is well-known, the basic physical magnitude which enables us to understand these phenomena is the bending energy of the amphiphilic layer situated between water and oil phases. A particularly interesting surfactant either from a basic or a technological point of view are the alkylglucosides (APG). In the synthesis, the glucose molecule (G) is attached to an alkyl chain alcohol [1]. In the APG molecule, the glucose is the hydrophilic part whereas the alkyl chain is the hydrophobic part.

---

*Corresponding author. Email: dkurlat@fi.uba.ar

Physics and Chemistry of Liquids
ISSN 0031-9104 print: ISSN 1029-0451 online
DOI: 10.1080/00319100420003035455

A remarkable feature of these compounds is that the sugar units of APG with water are independent of temperature changes. Hence, phase inversion is mainly dependent on their composition. On the other hand, this APG behaviour may be tuned by the presence of a cosurfactant [2–5]. We have studied the octane/water/glucoside/*n*-octanol microemulsion phase equilibrium at two different temperatures. In this study, our interest has been focused on the microscopic structure associated with the systems. In order to achieve this objective, we have used different experimental techniques i.e., Kerr effect, surface tension, light scattering and viscosity.

2. Materials and methods

2.1. *Materials*

In order to prepare the microemulsions, we have used octylglucoside (Akzo Nobel), filtered de-ionized water, *n*-octanol (Mallinckrodt) and octane (Riedel de Haven). All the components have been employed without further purification.

2.2. *Phase diagrams*

The liquid samples were placed in screw-capped, graduated Teflon-sealed tubes. The thermostatic control accuracy was of ±0.1°C. The liquid samples were placed in a water bath for a week. When equilibrium was reached, the phase volumes were measured with a 0.5 mL accuracy approximation. The composition of a quaternary mixture of water (W), oil (O), surfactant (S) and alcohol (A) is characterized by three independent composition variables which are determined by molar (or mass) fractions relations: $\alpha = [O]/([O] + [W])$, $\delta = [A]/([S] + [A])$ and $\gamma = ([S] + [A])/([O] + [W] + [S] + [A])$. These mass fractions are denoted by $[\cdot]$.

2.3. *Refraction index*

The refraction index of microemulsions (n_{MIC}) and the corresponding upper-phase refraction index (n_{SUP}) were measured in an ABBE refractometer, using a Na light source ($\lambda = 589$ nm). The temperature was 25.0 ± 0.5°C.

2.4. *Viscosity*

The microemulsion viscosity (η) was measured by means of a rolling-ball viscosimeter. The experimental results presented in this article were obtained by employing angles between 5 and 45° (by 5° steps) in a thermostatic bath (25.0 ± 0.5°C). In all the investigated systems, the observed viscosity was independent of the sphere velocity. Hence, it has been concluded that the samples were Newtonian liquids. The results presented in table 2 correspond to the mean viscosity values of all the measured angles. Errors are taken as the usual standard deviation.

2.5. *Light scattering*

The intensity of the scattered light was measured at angles in the range 25–90°. The light was perpendicularly polarized to the observation plane. The light source was a He–Ne laser beam of $\lambda = 632.8\,\mathrm{nm}$ and 15 mW power. To evaluate the geometrical parameters of the experimental set-up, benzene liquid samples were used ($n_b = 1.5029$ and $R_b = 7.7 \times 10^{-6}\,\mathrm{cm}^{-1}$ [6]). From these data, the Rayleigh factor (R) was determined for different microemulsions. In all the cases, it was observed that the R values were not angle dependent. The Rayleigh mean values are shown in table 2. The errors are estimated as the mean value standard deviation for different angles. On the other hand, self-correlation function of polarized light was determined. The observation angles are the same as the ones in the static case. By drawing a diagram of the self-correlation curve as a function of k^2 ($k = (4n/\pi\lambda)\sin(\theta/2)$), where n = solution solution refraction index and θ = observation angle, the first momentum was obtained. In all the cases, a linear relationship was obtained; the self-diffusion coefficient being given by the slope of the curve. The correlation coefficients were better than 0.998. The error indicated in table 2 corresponds to the statistical error that is deduced from the slope.

2.6. *Electric birefringence*

Our experimental set-up has already been described in previous papers [7]. An electrical square pulse applied to the electrodes in the Kerr cell was employed and the steady state Δn_s and signal relaxation $\Delta n(t)$ signals have been analyzed. It was verified that Δn_s is proportional to E^2. The Kerr constant (B) is defined as $B = \Delta n_s/(\lambda E^2)$. The relaxation time ($\langle\tau\rangle$) is calculated by fitting the normalized relaxation curve with a single exponential for each pulse of the applied tension. The field amplitudes ranged between 100 V and 1000 V and the square pulse width was never greater than 0.250 ms. The cell was 50-mm long and the distance between the electrodes was 2 mm. The source radiation was a He–Ne laser beam. Because these systems have a high conductivity, the time between each measurement was selected to be the longest in order to avoid heating the liquid samples. The mean relaxation time was obtained by averaging the relaxation time obtained for each single experiment and the evaluated error is the usual standard deviation.

3. Experimental results and discussion

The phase description of the mixture APG, water, octane and octanol is shown in figure 1. It can be observed that the well-known loop ("fish shape" in Kahlwelt's terminology [8]) can be observed as a function of the overall emulsifier concentration (γ) and the mixture relation for the emulsifiers (δ) for a fixed water/oil relation ($\alpha = 0.5872$). The symbol $\underline{2}$ indicates the lower microemulsion phase. If we move along the $\delta = 0.05$ line, for $\gamma \approx 0.35$ and $\gamma \approx 0.53$, the transitions for $\underline{2}$ to 3 and 3 to $\bar{2}$ are obtained respectively.

From $\gamma = 0.29$, the transition $\underline{2} \rightarrow 1 \rightarrow \bar{2}$ is obtained so the three equilibrium phases are changed into a single one. The contact point between the middle and the single phase (X) is called the "maximum synergy" point and for this temperature

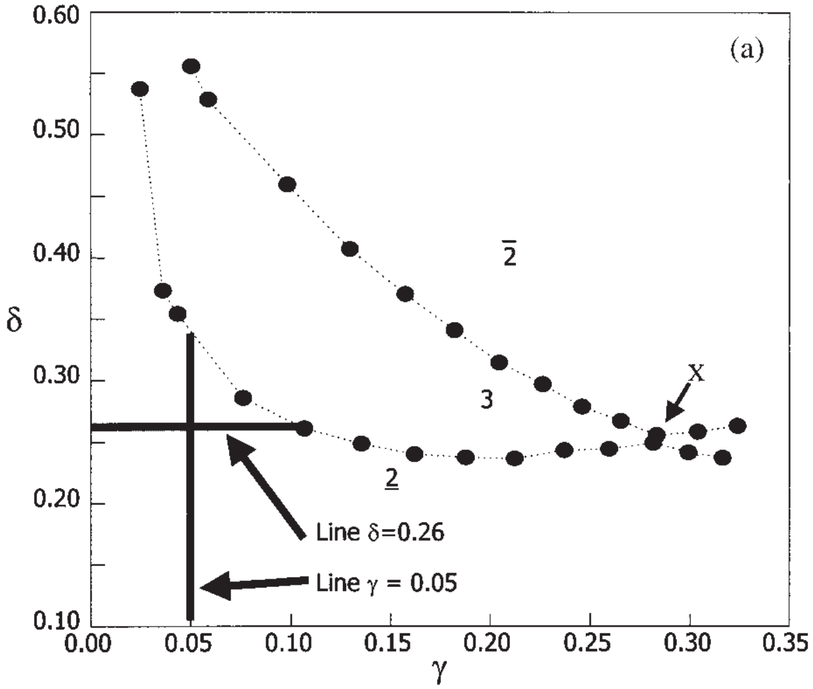

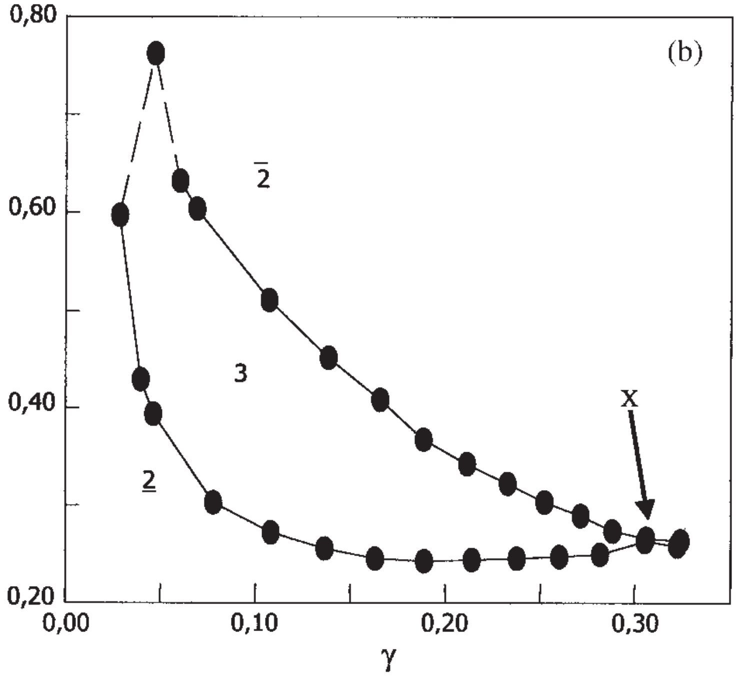

Figure 1. Equilibrium diagrams: (a) (25°C); (b) (50°C).

Table 1. Overall microemulsions composition. m_W, m_A, m_O, m_S are weight of water, *n*-octanol, octane and APG; V_{SUP} y V_{MIC} are upper and microemulsion volumes.

δ	γ	m_W (gr)	m_A (gr)	m_O (gr)	m_S (gr)	V_{SUP} (mL)	V_{MIC} (mL)
0.263	0.030	10.0028	0.1395	7.0315	0.3907	10.0	10.6
0.260	0.040	10.0041	0.1849	7.0315	0.5261	9.9	10.8
0.261	0.050	10.0154	0.2332	7.0315	0.6613	9.9	11.1
0.260	0.060	10.0015	0.2837	7.0315	0.8086	9.8	11.4
0.261	0.070	10.0046	0.3346	7.0315	0.9487	9.7	11.7
0.153	0.050	14.9876	0.2079	10.546	1.1471	14.9	16.5
0.199	0.050	15.0165	0.2696	10.548	1.0836	14.9	16.5
0.261	0.050	10.0154	0.2332	7.0315	0.6613	9.9	11.1
0.305	0.050	10.0125	0.2762	7.0322	0.6295	9.9	11.0
0.350	0.050	15.0068	0.4707	10.548	0.8761	14.9	16.5

Table 2. Experiment result $\Delta n_{SUP} = \Delta n_{MIN} = \pm 0.001$, $\Delta n = \pm 0.01$cp, $\Delta R = \pm 10\%$, $\Delta D = \pm 0.5 \times 10^{-11}\,\mathrm{m^2/s}$, $\Delta B = \pm 0.30 \times 10^{-13}\,\mathrm{m/V^2}$, $\Delta\tau = \pm 0.5\eta$s.

δ	γ	ϕ	n_{SUP}	n_{MIN}	η (cp)	R (cm^{-1})	D (m^2/s)	B (m/V^2)	τ (μs)
0.263	0.030	0.052	1.398	1.340	1.22	5.4×10^{-4}	3.82×10^{-11}	3.60×10^{-13}	1.2
0.260	0.040	0.078	1.397	1.344	1.58	11.0×10^{-4}	3.44×10^{-11}	4.63×10^{-13}	1.7
0.261	0.050	0.093	1.396	1.345	1.93	21.4×10^{-4}	3.40×10^{-11}	5.64×10^{-13}	2.5
0.260	0.060	0.118	1.398	1.349	2.40	34.3×10^{-4}	3.40×10^{-11}	6.58×10^{-13}	3.7
0.261	0.070	0.140	1.397	1.350	2.75	39.8×10^{-4}	2.63×10^{-11}	7.94×10^{-13}	4.8
0.153	0.050	0.091	1.396	1.346	1.77	5.1×10^{-4}	8.57×10^{-11}	0.63×10^{-13}	–
0.199	0.050	0.090	1.396	1.348	1.81	8.0×10^{-4}	4.71×10^{-11}	1.27×10^{-13}	2.0
0.261	0.050	0.093	1.396	1.345	1.93	21.4×10^{-4}	3.40×10^{-11}	5.64×10^{-13}	2.5
0.305	0.050	0.091	1.396	1.347	2.01	33.9×10^{-4}	2.70×10^{-11}	6.29×10^{-13}	3.5
0.350	0.050	0.092	1.394	1.345	2.50	82.9×10^{-4}	0.99×10^{-11}	13.50×10^{-13}	6.3

it reaches the values $\gamma = 0.29$ and $\delta = 0.25$. In the phase diagram achieved at 50°C, the X values are $\gamma = 0.31$ and $\delta = 0.26$. The phase diagrams are similar, which is a confirmation of the system stability with the temperature as stated by Rybinski [9].

Microemulsion structures in which $\delta = 0.26$ (horizontal line) and $\gamma = 0.050$ (vertical line) have been studied. In table 1, the microemulsion compositions (as mass components) and the phase volumes (V_{MIC}) in equilibrium with the upper ones (V_{SUP}) are shown.

It is necessary to estimate the phase volume fraction of the dispersed phase in the microemulsion ϕ. Due to the fact that the octane and the octanol are not dissolved in water, we assume that the dispersed phase is formed by the whole octane and octanol, which are not present in the upper phase, in addition to the whole APG. Under this hypothesis, ϕ is calculated by the following expression:

$$\phi = \frac{V_O + V_A + V_S - V_{SUP}}{V_{MIC}} \tag{1}$$

where V_O, V_A, V_S, V_{SUP} and V_{MIC} are the octane, octanol, alkylglucoside, upper-phase and microemulsion phase volumes. The results are presented in table 2. As be shown in this table, the refractive index measured in the upper phase is similar in all the samples and its value is identical to that of pure octane (1.369 ± 0.001). This shows that the quantity of dissolved alcohol in the upper phase is lower than the quantity that can be detected by refraction index measurements. Line $\delta = 0.260$: From table 2 data it can be shown that there exists a linear relationship between n_{MIC} and ϕ ($n_{\mathrm{MIC}} = 0.25\gamma + 1.333$) and between ϕ and γ ($\phi = 2.16\gamma - 0.012$). The composition of the microemulsion changes with the total surfactant proportion. The Kerr constant of the micellar systems depends on the volume fraction occupied by the micellar systems and their shape and size. When the dependence of Kerr constant on ϕ is analyzed, it is observed that the linear correlation coefficient is 0.997. Hence, it can be concluded that micelle shape and form have not changed along this line.

On the other hand, Rayleigh factor measurements also show a linear relation $R\ (\mathrm{cm}^{-1}) = 421 \times 10^{-4}\phi - 17.7 \times 10^{-4}$. Because the Rayleigh factor of a system is always positive, any dissolved surfactant content may be present in the continuous medium. So, the surfactant volume fraction which is not into the micelles is $\phi_1 = 0.044$. The volume fraction which is occupied by the micelles $\phi_p = \phi - \phi_1$.

The translation diffusion coefficient of a micellar system depends on the volume fraction as [10]:

$$D = D_o(1 + b\phi_p) \tag{2}$$

where b is a function of the interactions between the micelles and ϕ_p is the volume fraction of the nanodroplets. From table 2 data, the D dependence on ϕ_p is negligible. Hence, we can accept that the structures, shape and size are not dependent on the value and the interactions between them are very small.

On the other hand, the self-diffusion coefficient may be related to the hydrodynamic radius (R_h) by using the Debye–Stokes–Einstein relationship:

$$D = k_B T / 6\pi\eta_o R_h \tag{3}$$

where T is the temperature, η_o, the continuous medium viscosity and k_{B}, the Boltzman's constant. The nanodroplets mean hydrodynamic radius is $R_h = 5.0 \pm 0.5\,\mathrm{nm}$.

The viscosity of a micellar suspension may be described as a function of the fraction, which is occupied by the micelles in the continuous medium. By assuming that the viscosity continuous medium is η_0, the microemulsion viscosity is [11]:

$$\eta = \eta_0(1 + \nu\phi_p) \tag{4}$$

where ν is a function of the volume and the ellipsoidal nanodroplet axial relation. It was determined that the η_0 value is 1.09, by measuring the viscosity of an APG and water molecular solution at the $\phi_o = 0.044$ concentration. From the experimental data, the result can be described by the equation (4) with $\nu = 15.4 \pm 1.1$. In this case the micelles can be modelled as ellipses of revolution, the value which is deduced of ν [11] is $a/b = 10$ approximately and $a = (18.4 \pm 1.8)\,\mathrm{nm}$.

Birefringence relaxation times are not constant, because it grows with ϕ which is indicative that the result interpretation is incomplete. This can be explained by the fact that polydispersion increases when the system is near the phase transition zone. Line $\gamma = 0.050$: from the table 2 data it can be shown that the microemulsion refraction index is $1.346\,(\pm 0.001)$ and $\phi = 0.090$; then, the microemulsions compositions are

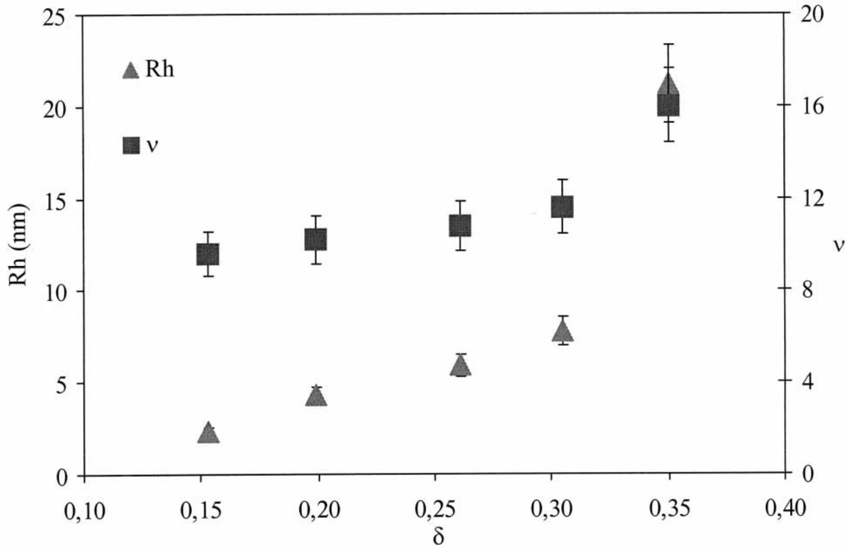

Figure 2. Simha factor (ν) and hydrodynamic radius (R_h) as a function of δ.

almost the similar. As can be appreciated from table 2, the Rayleigh factor, the Kerr constant and the viscosity increases with δ in a non-linear form, in spite of ϕ remaining practically unchanged. Simultaneously, the diffusion coefficient diminishes with δ. All these results show that the micelle structure changes with δ.

To estimate the micelle shape, we assume that the continuous medium surfactant concentration (under a monomer form) is the one which we have calculated previously. So, by applying viscosity measurements and equation (4), ν for each sample can be calculated. By using equation (3) the R_h value of each sample is calculated. The results are shown in figure 2.

The size of the micelles can be estimated by employing the Simha factor and the hydrodynamic radius equation:

$$R_h = a\sqrt[3]{p^2}\,\frac{\sqrt{1-p^2}}{\log\left(\left(1+\sqrt{1-p^2}\right)/p\right)} \tag{5}$$

The results presented in figure 3 are normalized with respect to line $\delta = 0.260$; it shows that the micelles change in their size, but not the shape, with δ. This indicates that alcohol, does not affect interface properties, whereas the curvature is changed.

Conclusions

We have established that the surfactant (APG) is dissolved in water as a monomer and its concentration is 0.044. This value is independent of the ratio alcohol/APG. The micelles are not spherical. Their eccentricities are nearly independent of the ratio alcohol/APG. We have assumed a revolution ellipsoidal form and deduced

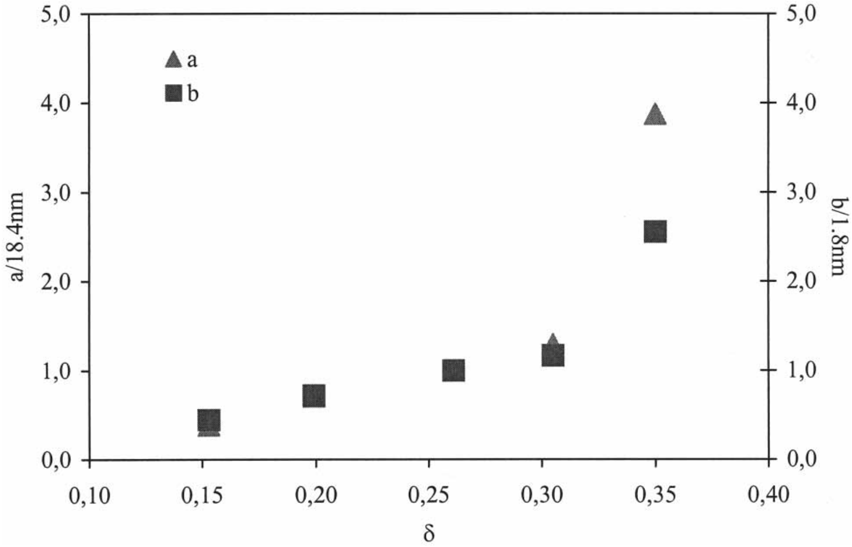

Figure 3. (a) Mayor semiaxis and (b) minor semiaxis of revolution ellipsoids as a function of δ.

an axial ratio $a/b = 0.1$. This corresponds to an eccentricity $e = (1 - (b/a)) = 0.995$. This relation changes close to the phase-transition concentration. The micelle size increases with the ratio alcohol/AG. This behaviour becomes significantly closer to the phase-transition zone.

References

[1] R. Eskuchen, M. Nitsche, Alkyl polyglucosides, In *Technology*, *Properties and Applications*, Chap. 2, K. Hill, W. von Rybinski, G. Stoll (Eds.), p. 12, VCH Publishers, New York (USA), Weinheim (Germany) (1997).
[2] M. Kahlweit, R. Strey, G. Busse, *J. Phys. Chem.*, **95**, 5344 (1991)
[3] T. Sottmann, K. Kluge, R. Strey, *Langmuir*, **18**, 3058 (2002).
[4] B. Ginzberg, S. Bergerman, D. Kurlat, *Phys. Chem. Liq.*, **27**, 83 (1992).
[5] J. Reimer, O. Söderman, T. Sottmann, K. Kluge, R. Strey, *Langmuir*, **19**, 10692 (2003).
[6] H. Wahid, *Phys. Chem. Liq.*, **26**, 15 (1993).
[7] E. Acosta, D.H. Kurlat, M. Bisceglia, B. Ginzberg, L. Baikauskas, S.D. Romano, *Colloids Surfaces A: Physicochem. Eng. Aspects*, **106**, 11 (1996).
[8] M. Kalweit, R. Strey, *Angew. Chem. Int. Ed. Engl.*, **94**, 3881 (1994).
[9] W. Von Rybinsky, B. Guckenbiehl, H. Tesmann, *Colloids and Surfaces A*: *Physicochem. Eng. Aspects*, **142**, 333 (1998).
[10] J.M. Schurr, *CRC Critical Review in Biochemistry*, November, 371 (1977).
[11] C. Tanford, *Physical Chemistry of Macromolecules*, Chap. 6. p. 335, John Wiley and Sons (1965).